JOINT INSTITUTE FOR NUCLEAR RESEARCH

PROCEEDINGS OF THE 1987 JINR-CERN SCHOOL OF PHYSICS

(A.O.N.S.U. near Varna, Bulgaria, 6-19 September 1987)

E1,2-88-426

ТРУДЫ ШКОЛЫ ОИЯИ-ЦЕРН ПО ФИЗИКЕ 1987

(А.О.Н.С.У. под Варной, Болгария, 6-19 сентября 1987 года)

Dubna 1988

THE JINR SCIENTIFIC PROGRAMME

A.N.Sissakian
Joint Institute for Nuclear Research, Dubna

1. INTRODUCTION

The Joint Institute for Nuclear Research was established more than 30 years ago, in March 1956, as an international scientific center, on the basis of two soviet scientific laboratories. One of them disposed of the 680 MeV synchrocyclotron which operated since 1949. In the other one the construction of the 10 GeV synchrophasotron was in the final stage. The Dubna synchrophasotron was put into operation in 1957.

At present 11 member states: Bulgaria, Hungary, Vietnam, The German Democratic Republic, The Korean People's Democratic Republic, Cuba, Mongolia, Poland, Romania, USSR and Czechoslovakia contribute to the Institute. JINR employes more than one thousand scientists, more than six thousand people work in its laboratories and departments; about one thousand and a half visiting scientists come annually to work in Dubna.

The supreme body of the Institute is the Committee of Plenipotentiaries of the governments of Member States which is convened annually and considers the major problems of the Institute's activity.

The Finance Committee is concerned with the annual budget, contributions from the member states, etc.

The Scientific Council which is convened twice a year determines the research policy of JINR. The Council submits its recommendations on planning and finances, construction of new facilities, etc., to the Committee of Plenipotentiaries. The Council has three sections: High Energy Physics, Low Energy Physics and Theoretical Physics. The Council sections have specialized subcommittees which are concerned with research techniques.

Table 1 shows the structure of the Joint Institute governing bodies.
The JINR Directorate is reelected each three years. Now the Director of the Institute is the distinguished Soviet physicist and mathematician Academician N.N.Bogolubov.

Table 1

JINR ADMINISTRATION (JINR governing bodies)

ADMINISTRATION: STRUCTURE AND MEMBERSHIP

COMMITTEE OF PLENIPOTENTIARIES

FINANCE COMMITTEE

SCIENTIFIC COUNCIL

Chairman - Academician N.N.Bogolubov
Co-Chairman - Professor E.Entralgo
Co-Chairman - Professor M.Gmitro
Chief scientific secretary - Professor A.N.Sissakian

Bulgaria	Hungary	Vietnam Socialist Republic	German DR	Korean People's DR	Cuba	Mongolia	Poland	Romania	USSR	Czechoslovakia

SC section on High Energy Physics			SC section on Theoretical Physics	SC section on Low Energy Physics		
Chamber Committee	Electronic Experiments Committee	Photoemulsion Experiments Committee		Neutron Physics Committee	Nuclear Structure Committee	Heavy ion Physics Committee

Table 2

THE STRUCTURE OF THE INSTITUTE. SCIENTIFIC PROGRAM OF THE JINR LABORATORIES

JOINT INSTITUTE FOR NUCLEAR RESEARCH STRUCTURE AND RESEARCH ACTIVITIES

DIRECTIRATE

Director - N.N.Bogolubov
Vice-director - E.Entralgo
Vice-director - M.Gmitro

Laboratory of Theoretical Physics	Laboratory of High Energy Physics	Laboratory of Nuclear Problems	Laboratory of Nuclear Reactions	Laboratory of Neutron Physics	Laboratory of Computing Technique & Automation	Main Divisions
Director - V.G.Kadyshevsky Research activities: - elementary particles; - atomic nucleus theory; - condensed matter theory	Director - A.M.Baldin Research activities: - nucleon structure; - strong interactions; - resonant states; - electromagnetic interactions	Director - V.P.Dzhelepov Research activities: - strong, weak, el/m interactions; - search of new particles; - nuclear structure	Director - G.N.Flerov Research activities: - search of superheavy elements; - transuranium isotopes; - complex nuclei interactions	Director - I.M.Frank Research activities: - neutron spectrometry; - neutron basic properties; - nuclear structure & dynamics of solid & liquid matter; - light nuclei reactions	Director - M.G.Meshcheryakov Research activities: - computation; - auto-systems for chamber film procession; - computer equipment of experimental facilities; - software systems	Division of New Methods of Accelerating Serpukhov Scientific Experimental Division Division of Chief Scientific Secretary Scientific & Technical Information Service Experimental Physics Facilities Division

Table 3

JINR SEARCH FACILITIES

I. SYNCHROPHASOTRON

1. Injector - duoplasmatron source
   - energy - 10 GeV
   - intensity - $4\cdot10^{12}$ proton/cycle
   - $1\cdot10^{12}$ deutron/cycle
2. Injector - polyrized deuteron source
   - energy - 4.2 GeV/nucleon
   - intensity ~ $1\cdot10^{9}$ deuteron/cycle
   - degree of polyrization ~ 50%
3. Injector - laser source, KRION - source
   - energy - 4,2 Gev/nuclon
   - beam intensity per cycle:

^{6}Li - $1.5\cdot10^{8}$	^{19}F - $1.5\cdot10^{7}$
^{7}Li - $4\cdot10^{9}$	^{22}Ne - $1\cdot10^{4}$
^{12}C - $2\cdot10^{9}$	^{24}Mg - $3\cdot10^{7}$
^{16}O - $5\cdot10^{7}$	^{28}Si - $3\cdot10^{4}$

II PHASOTRON

- energy - 680 MeV
- intensity - $4\cdot10^{13}$ proton/cycle

III CYCLOTRONS

1. Heavy ion cyclotron U-300
   - energy of accelerated particles - 250 Z^2/A MeV
   - mass/charge A/Z - 4.5÷7
   - intensity - $10^{11}\div10^{14}$ particle/sec
2. Heavy ion cyclotron U-400
   - energy of accelerated particles - 650 Z^2/A MeV
   - mass/charge A/Z - 4÷20
   - intensity - $10^{12}\div10^{14}$ particle/sec
3. Microtron MT-25
   - energy of electrons - 25 MeV
   - averyge current - 20 mkA
   - pulsed current - 20 mA
   - pulse duration - 2.3 microsec

IV. FAST NEUTRON PULSED REACTORS

1. IBR-30
   - average heat output - 30 kW
   - output per pulse - 150 mW
   - pulse duration ~ 50 microsec
   - intensity - $5\cdot10^{14}$ neutr/$cm^2\cdot$sec
2. IBR-2
   - average heat output - 2 M.W.
   - output per pulse - 1350 M.W.
   - pulse duration - 230 microsec
   - intensity - 10^{16} neutr/$cm^2\cdot$sec

The present Vice-directors are Professor Elias Entralgo from Cuba, responsible for research in High Energy Physics, and Professor Marian Gmitro from ČSSR, responsible for research in Low Energy Physics. Professor Yu.N.Denisov is appointed as Administrative Director.

JINR has 6 laboratories, each equivalent to a rather large institute and associated departments. Table 2 shows the structure of the JINR's laboratories and the subjects of their research.

As you see, the scale of scientific work at JINR is broad. The Joint Institute is one of the unique centres where almost all branches of nuclear science are developed, namely, research in HEP, in physics on condensed matter, in neutron physics, theoretical physics, nuclear instrumentation and methods. There are large possibilities to enrich the research in various applied sciences. Table 3 presents the main facilities of the Institute to perform different investigations.

As I already mentioned, one of the principle trends of the JINR scientific programme is research in high energy physics. The experiments are carried out mainly at the Serpukhov proton-synchrotron and CERN's accelerators.

In 1970 in Dubna Academician A.M.Baldin proposed to develop a new branch of the nuclear physics - the so-called relativistic nuclear physics which by its goals and problems is close to high energy physics.The investigations in this field are performed at the JINR synchrophasotron and now are considerably enlarged.By the end of 1988 the construction of a new accelerator of relativistic nuclei on superconducting magnets is forseen.This new machine - NUCLOTRON - may be used also as the injector for a SuperNUCLOTRON with the energy 60 GeV per nucleon and further developed into a collider.

A number of the elementary particle experiments are carried out at the JINR low energy facilities, particularly, at the Dubna neutron impulse reactor IBR-2.
The principal investigations in low and intermediate energies will be performed with the help of the reconstructed phasotron and meson factory of the Institute of Nuclear Physics of the USSR Academy of Sciences in Troitzk. These will be the main research facilities in this range of energies up to 2000.

2. EXPERIMENTS CARRIED OUT AT THE SERPUKHOV PS

More than 20 years JINR collaborates successfully with the Institute of High Energy Physics in Protvino. 25 large experimental installations of the Institute were used for experimental research at the Serpukhov 70 GeV PS.

At present the Serpukhov machine has started to operate with the booster. The great part of the PS operational time is used for the JINR experiments. Table 4 illustrates the principle information about the JINR experiments which are carried out at the Serpukhov PS.

Table 4 . EXPERIMENTAL FACILITIES USED AT THE SERPUKHOV PS

BIS-2 Diffraction Spectrometer with proportional chambers; angle resolution: 0.2-0.4 mrad; mass resolution: 2-5 MeV (put in operation in 1978)	Search for charmed and narrow baryon resonanses: Charmed baryon have been registered via the decays $\Lambda_c^+ \to \bar{K}^0 p \pi^+ \pi^-$ (1); $\Lambda_c^+ \to \Lambda^0 \pi^+ \pi^+ \pi^-$ (2); $\sigma \cdot B(1) = 60 \pm 15$ μb per nucleon. New baryon resonance found $N_\phi \to \Sigma^-(1385)K^+$; $M_{N\phi} = 1956 \pm 8$ MeV/c^2; $\Gamma_{N\phi} = (27 \pm 15)$ MeV/c^2
HYPERON Missing Mass Spectrometer (JINR-IHEP) Spark and proportional chambers: Shower electron and γ-quanta detectors (put in operation in 1978)	Study of multiparticles processes and binary $\pi^- p^+ \to K^+ \Sigma^+ \Sigma^+_{1385}$; Hyper charge exchange reactions at 12 GeV; Decays of K^+- and K^0-mesons.
LUDMILA Hydrogen Chamber Volume: 860 l; track sensitive internal target of 10 l filled with liquid deuterium put in operation in 1976 and from now being out of use	Investigation of the $\bar{d}$ - d interactions
POLARIMETER (JINR-IHEP) Spectrometer with a "frozen" polarized proton target; proportional chambers (put in operation in 1976)	Investigation of the polarization effects in the hadron-hadron collisions in a broad range of momenta transfered at the energies up to 60 GeV
POSITRONIUM Magnetic Sperctometer with a drift chambers (put in operation in 1982)	Study of the reaction $\pi^0 \to \gamma + (e^+e^-)$-atom relativistic positronium interaction with matter
MIS-2 Magnetic Spark Spectrometer with film data taking; proportional chambers and scintillation counter trigger system	Investigation of the bozon resonances in the dissociation processes of meson on nuclei. The mass and the width of the radial excitations of the π-meson has been determined: $M_{\pi'} = (1240 \pm 30)$ MeV; $\Gamma = (360 \pm 120)$ MeV and $M_{\pi''} = (1770 \pm 30)$ MeV; $\Gamma = (310 \pm 50)$ MeV
SIGMA-AJAX Magnetic Spectrometer (JINR-IHEP) spark and proportional chambers; gamma spectrometer on lead glass (put in operation in 1980)	The first time the compton effect on π^--meson has been investigated. Polarizability of the pion in the external field found; fundamental constant $\alpha_\pi = (6.8 \pm 1.4) \cdot 10^{-43}$ cm^3 was determined as well. Coupling constant $\gamma \to 3\pi$ was measured for the first time, $F^{\gamma 3\pi} = 13.0 \pm 0.5$, the result confirming the chiral anomaly hypothesis.
NEUTRINO DETECTOR (JINR-IHEP) target-calorimeter; muon spectrometer; vertex detector; shower detector of e^- and γ-quanta (put in operation in 1985)	The cross section production, life time and decay modes of the short lived particles in the beam of muon neutrinos. Weak current structure; deep inelastic scattering of neutrinos on nucleons.

2.1 The joint IHEP-JINR experiment carried out with the "Polarimeter" set-up

This installation is designed to investigate polarization effects in the π^--meson-proton interactions at 40 GeV/c. The large hydrogen polarized target (40 cm in length) of the "frozen" type was used in this experiment.

The systematic study of the polarization effects in the binary reactions

$$\pi^- p \to \pi^0 n; \quad M^0 n; \quad K_s^0 \Lambda; \tag{1}$$

where $M = \eta, \eta', f, \omega$,

was performed by using the "POLARIMETER" set-up. The polarization P versus to the momentum transferred in different reactions is shown in Fig.1. It is seen that even at the energy of 40 GeV/c the polarization effects are large (they reach 30-40% in a few cases) and the dependence of the polarization from the momentum transferred has a complicated character. The naive quark models predict the extinction effects with the energy increasing; they cannot describe the experimental data obtained and contradict totally the polarization effects observed in inclusive processes. A significant azimuthal asymmetry has been found in the inclusive reaction $\pi^- p \to \pi^0 + X$ for large P_t in the central region ($X \sim 0$).

2.2 The joint JINR-IHEP experiment carried out with the HYPERON spectrometer

- The study of the η, K_s^0 and K^0 meson inclusive production in the π^+-K^+ meson interaction with 6 nuclei has been performed at 10 GeV. Some interesting results were found in the analysis of the differential cross section ratio

$$R_A(x_F) = \frac{d\sigma}{dx_F}(\pi^+ A \to \eta x) \Big/ \frac{d\sigma}{dx_F}(\pi^+ d \to \eta x).$$

It was found that this ratio increases with the rise of X_F (see Fig.2). This fact contradicts the Glauber model according to which R_a is not dependent from X_F. The account of the hadron formation length $l_f = \frac{P_0}{\chi}(1-X_F)$ contradicts also the experimental results if one uses as the coefficient of the string tension χ the value obtained from the slope of Regge trajectories $\chi = 1$ GeV/fm. It may be concluded that tension coefficient of the colour triplet string is at least more than 3 GeV/fm ($\chi > 3$ GeV/fm) at these energies.

More detailed analysis showed that the observable dependence R_a might be explained by different screening in the nuclei contributions from 3-reggeon diagrams. The differential cross sections of quasi binary processes of the type $\pi^+ A \to K^+ Y + A'$ on deuterium and carbon were measured at 10 GeV. It was found that the effective number of nucleons A_{eff} (t) is increased with the increasing of the momentum transferred t. This contradicts the Glauber model and agrees well with the predictions of the model which takes into account the effects of the colour screening.

- The most strong limitation of the probability of the electroweak decay K_s^0 e^+e^- prohibited by the standard model was obtained in this experiment

$$BR(K_s^0 \to e^+e^-) \leq 1,1 \cdot 10^{-4} \quad (90\ C.L.).$$

"POLARIMETER" "HYPERON"

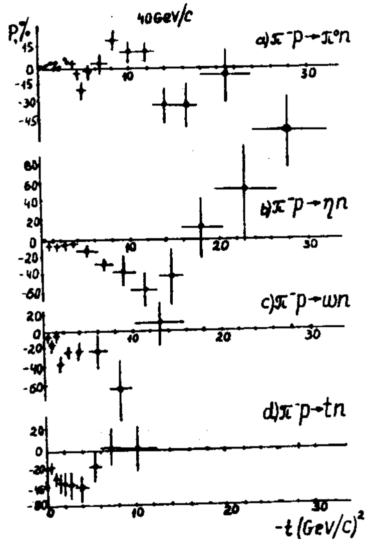

Fig. 1.

Study of the polarization effects in

$$\pi^-p \to \begin{cases} \pi^0 n \\ M^0 n \\ K_S^0 \Lambda \end{cases}, \; M=\eta,\eta',f,\omega .$$

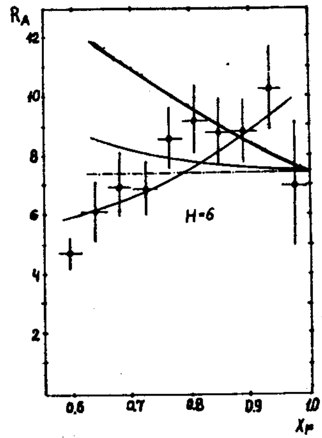

Fig. 2.

Hadron formation length

$$\ell_f = \frac{P_0}{\varkappa}\,(1 - X_F)$$

$\varkappa$ - string tension.

2.3. The joint IHEP-JINR-CERN experiment carried out with the SIGMA-AJAKS spectrometer

The processes of the pion pair production by 40 GeV pions near threshold in the Coulomb field of nuclei have been studied in this experiment

$$\pi^- + A \to \pi^- + \pi^0 + A .$$

The cross section of such reactions was determined for nuclei C, Fe, Al in the Coulomb field with $t < 10^{-3}(GeV/c)^2$ and small invariant masses of the system ($\pi^-\pi^0$). This allowed to determine the constant of the fundamental processes $\gamma \to 3\pi$ equal to $F^{3\pi} = (12,9\pm0,9\pm0,5)GeV^{-3}$. The experimental value obtained is in a good agreement with the theoretical prediction of $F^{3\pi} = (10.5 \pm 1.5)GeV^{-3}$ which was made in the low energy limit of QCD with the Weiss-Zumino-Vitten chiral lagrangian taking into account the hypothesis of chiral anomalies that bounds together amplitudes of processes $\gamma\to 3\pi$ and $\pi^0\to 2\gamma$. Thus, for the first time the hypothesis of chiral anomalies was experimentally confirmed.

The inclusive reaction of the cumulative proton emission in 40 GeV/c π^-, K^-, $\bar{p}$ - interactions with Be nuclei was investigated in the SIGMA-AIAKS experiment. The differential cross-sections versus the kinetic energy of the cumulative proton were measured in the range 0,1 ÷ 0,3 GeV. The averaged inclusive cross-sections ratios for different types of the incident particles were obtained:

$F_K/F_\pi = 0,98 \pm 0,05 \pm 0,01$

$F_{\bar{p}}/F_\pi = 2,12 \pm 0,16 \pm 0,05.$

An interesting result is the high value of $F_{\bar{p}}/F_\pi$. The average values of the inclusive cross-sections normalized by the inelastic nuclear cross-sections with beryllium are also of interest:

$$\frac{F_K/\sigma^K_{ABS}}{F\ /\sigma^\pi_{ABS}} = 1.06 \pm 0.05_{STAT} \pm 0.01_{SYST}$$

$$\frac{F_{\bar{p}}\ /\sigma^{\bar{p}}_{ABS}}{F_\pi\ /\sigma^\pi_{ABS}} = 1.40 \pm 0.10_{STAT} \pm 0.03_{SYST}\ .$$

Thus the probability to produce a cumulative proton in the process of a nuclear interaction is equal within experimental errors for kaons and pions, but for antiprotons this probability is 1.4 times higher.

2.4. The filmless spark chamber spectrometer BIS-2

In the experiments carried out by using the spectrometer BIS-2 a meson resonance with a negative strangeness U(3100) produced in neutron-nuclei interactions at the mean neutron momentum of 40 GeV/c was observed. Carbon, Aluminium and Cuprum were used as nuclear targets. Spectra of invariant masses plotted for events consisting of Λ^0 and $\bar{p}$ and charged pions or K^0_s, p, $\bar{p}$ and charged pions were analysed to search U(3100). Λ^0 and K^0_s were identified according to their decays into $p\pi^-$ and $\pi^+\pi^-$ among reconstructed neutral prongs. A total number of ~ 8,5 x 10^4 events with Λ^0 and 4,5 x 10^4 with K^0_s were identified. Among Λ^0 events the spectra of invariant masses were analysed for configurations corresponding to possible decays:

$$U^+ \to \Lambda^0\bar{p}\pi^+\pi^-\ (1);\quad U^0 \to \Lambda^0 p\pi^+\ (2);$$

$$U^0 \to \Lambda^0\bar{p}\pi^+\pi^+\pi^-(3);\quad U^- \to \Lambda^0\bar{p}\pi^+\pi^-(4);\quad U^{--} \to \Lambda^0\bar{p}\pi^-(5).$$

The summed spectrum obtained for all invariant mass configurations (1-5) is presented in Fig.3. The peak in the region of masses 3030 ÷ 3090 MeV/c^2 corresponds to ~ 130 events of U(3100) above background level (~ 270 events) that corresponds to the statistical quantity of more than 8 standard deviations. Among these events the great part consisting of about 75 events is due to the decays into the channel (2). The detailed analysis showed that two-particle decay $U^0 \to \Lambda^0\Delta(1700)$ (6) occurred through which a half of all observed decays were realised.

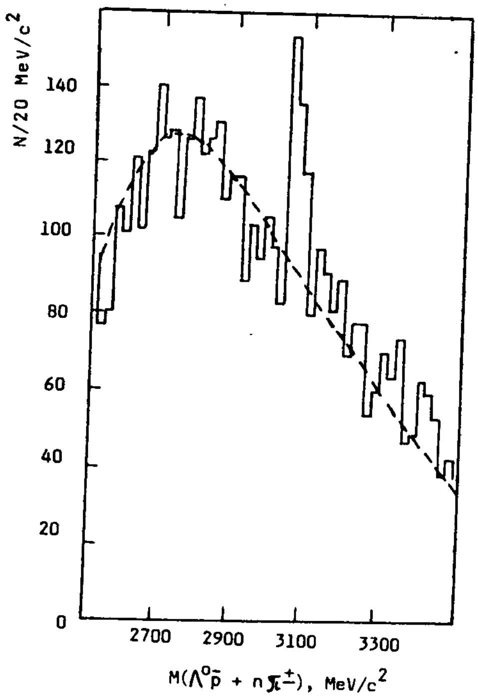

Fig. 3.

B I S - 2

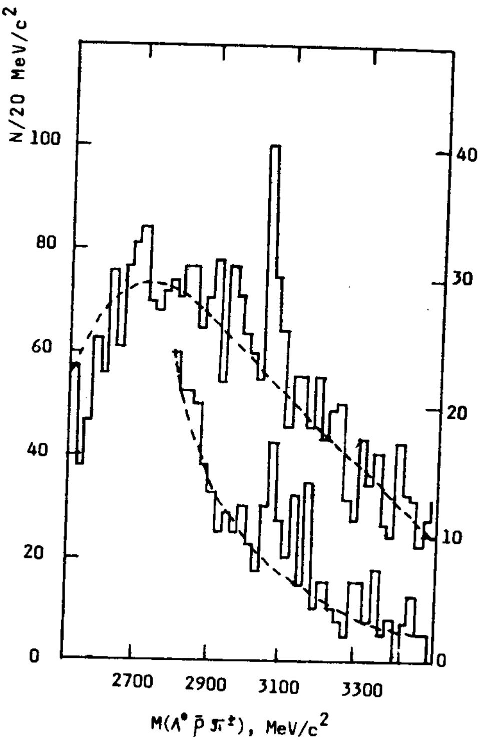

Fig. 4.

The summed spectrum obtained for all invariant mass configurations:

$U^{+} \to \Lambda^{0}\bar{p}\pi^{+}\pi^{-}$, $U^{0} \to \Lambda^{0}\bar{p}\pi^{+}$

$U^{0} \to \Lambda^{0}\bar{p}\pi^{+}\pi^{+}\pi^{-}$, $U^{-} \to \Lambda^{0}\bar{p}\pi^{+}\bar{p}$

$U^{--} \to \Lambda^{0}\bar{p}\pi^{-}$.

From the analysis of spectra $\Lambda^0 \bar{p} \pi^+$ (see Fig.4) for events recorded in the exposures with C, Al, Cu targets the A-dependence of U(3100) is determined which is characterized by the value of the power index $\alpha = 0.6 \pm 0.3$ within $\sigma \sim A^{\alpha}$ parametrization. The spectrum of the system $K^0_s\, p\bar{p}\pi^+$ invariant masses was reconstructed for events consisting of K^0_s. In this case, in the interval of masses 3030 ÷ 3090 MeV/c^2 there is a peak which consists of ~ 50 events over the background level. The presence of such a peak prooves the availability of decays $U^+ \to \bar{K}^0_s p\bar{p}\pi^+$ and $\bar{U}^+ \to K^0_s p\bar{p}\pi^+$.
Thus, approximately 180 events of the narrow resonance production ($\Gamma \leqslant 20$ MeV/c^2) were recorded. This resonance has a negative strangeness and decays into baryon, antibaryon and meson. The average value of the resonance mass is M=(3068± 40)MeV/c^2. New channels of the U(3100) decay into $\Lambda^0 \bar{p}\pi^+$; $\Lambda^0\Delta$ (1700); $\Lambda^0 \bar{p}\pi^-$; $\bar{K}^0 p\bar{p}\pi^+$ were observed for the first time.

The isotopic spin of the resonance is 3/2. The product of the resonance cross section in the region $X_F > 0.5$ and probability of its decay into each available channel is equal from 1 to 10 mkb per nucleus of C. To describe principle properties of the resonance obtained within quark structure model one needs four valence quarks at least.

During last decade great attention is paid to the study of the polarization of hyperons produced in the inclusive reactions. A number of theoretical models explain the polarization as the result of the quark spin-orbit interaction in a field of forces which bound them into hadrons. Therefore one of the important tendencies of investigations performed with the help of the BIS-2 spectrometer is the study of the polarization effects. In the 1986 in the experiment carried out at the Serpukhov PS, the polarization of Ξ^- - hyperons produced by inclusive neutrons at the mean momentum of 40 GeV/c^2 was measured. The hyperons were registered by the cascade decay:

$$\Xi^- \to \Lambda^0 + \pi^- \quad \Lambda^0 \to p + \pi^-.$$

A total number of $\sim 1.6 \times 10^5$ decays of $\Lambda^0 \to p\pi^-$ was identified. To study the polarization Ξ^- - 1267 events of hyperons from the interval of masses $M(\Xi^-) =$ (1321.3 ± 8) MeV/c^2 were analysed. The kinematical region of registration of Ξ^- hyperons is $0 < P_\perp < 1.3$ GeV/c, $\langle X_F \rangle = 0.45$. It is seen from the analysis that Ξ^- - hyperons produced in such conditions are polarized negatively ($\mathcal{P} = -0.3 \pm 0.2$) longitudinally to the plane of their production which is determined by the vector product of the primary neutron and Ξ^- hyperon moments in the laboratory system. The parameter of the asymmetry decay is $\Xi^- \to \Lambda^0\pi$: $\alpha(\Xi^-) = -0.43 \pm 0.16$. The polarization of Ξ^- agrees with the polarization of Λ^0 , measured in the same experiment, as well as with the polarization of produced by the 40 GeV/c protons, but is opposite by sign to the polarization of Ξ^- produced by the 5GeV/c negative kaons.

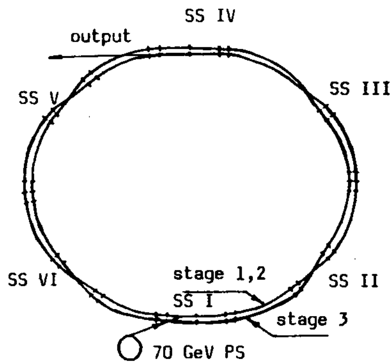

Fig. 5. The scheme of the UNK magnet structure.

2.5. The perpectives of experimental research at the Serpukhov UNK *)

The programme of the experiments in High Energy Physics is based on the development and construction of the accelerating complex - UNK - at IHEP. Fig.5 shows tha general scheme of this complex designed to get the energy of 3000 GeV or 3 TeV. The construction of this complex will proceed in a few stages:

- UNK-1 provides the acceleration of 400-600 GeV protons in a warm ring. In 1990 the first experiment by using the internal jet target will be carried out. This will be the joint IHEP-JINR-CERN experiment which is called "PARUS-NEPTUN". Now the experimental set-up is designed and manufactured.

- UNK-2 is planned to put in operation in 1993. The protons will be accelerated up to the energy of 3 TeV in a cryogenic ring. By this time a number of experiments in the extracted beams will be prepared, including the experiment which will be perperformed by using the multiparticle hadronic spectrometer ("MARS-MPS").

- The third stage is the construction of the UNK-3 complex - pp colliding beams with the energy of 3 TeV which must be constructed by 1995. The Joint Institute is going to participate at these experiments by constructing a universal calorimeter of new type (UCD - Universal Calorimeter Detector).

Most interest is centered on the experiments which will investigate:

- the heavy B-particles;
- phenomena in pure hyperon beams;

---

*) See N.E.Tyurin. "Accelerating and Storage Complex (UNK) Experimental Research Programme".
Talk given at the ICFA Seminar at Brookhaven "Future Perspectives in High Energy Physics" (6-10 October,1987).

- search for "glueballs" and study of their production;
- specific phenomena in the experiments with high energy polarized protons;
- the universality of ν_μ, ν_e, ν_τ interactions.

3. JOINT EXPERIMENTS AT THE CERN AND FNAL ACCELERATORS

3.1. The joint CERN-JINR experiment PS-179

The experimental set-up is designed to study the low antiprotons interactions with nuclei. The experiment was carried out at the antiproton beams of the LEAR (CERN).

The probability of the annihilation of antiprotons stopped on the neutron and proton bound in ^3He and ^4He nuclei was determined for the first time. The ratio of these probabilities $R = W_n/W_p$ was $R = 0.35 \pm 0.07$ in the case of the ^3He annihilation and $R = 0.48 \pm 0.1$ in the case of the ^4He annihilation. This value is almost two times lesser than the value $R = 0.82 \pm 0.03$ of the corresponding ratio of the possible annihilation of antiprotons on free nucleons. This discrepancy can be explained by probabilities.

The interesting effect was discovered in the study of Λ and K^0_s meson production in the interaction of antiprotons with the neon nuclei at 600 MeV/c. It was found that the production of Λ - particles was two times greater than the production of K^0_s mesons while in the elementary p-N annihilation the situation is opposite, that is the K^0_s meson production is 5 times greater than the cross section of Λ - particles production.

3.2. The NA-4 experiment

A number of new results are obtained in the NA-4 experiment performed by the Bologna-CERN-Dubna-Münich-Saclay collaboration. This experiment is designed to study a nucleon structure using the deep inelastic scattering of muons from various nuclei. Data are collected from hydrogen, deuterium, carbon, nitrogen and iron targets.

- New results are reported on nuclear effects in structure functions known as the EMC effect. The ratio of nucleon structure functions measured from iron and deuterium targets, $F_2^{Fe}(x,Q^2)/F_2^D(x,Q^2)$ is determined as a function of x and Q^2 in the kinematical region x = 0.06-0.8, Q^2= 14-70 GeV^2. A special attention has been paid during data collection and analysis to minimize possible systematic errors. As the result, statistical and systematical errors of F_2^{Fe} do not exeed 2%. No Q^2 dependence of $F_2^{Fe}(x, Q^2)$ is observed (see Fig.6). Averaged over Q^2 range the ratio $R_{Fe}(x)$ in the region $x > 0.3$ has the same behaviour as previously observed by the EMC, NA-4 and other experiments (see Fig.7).But at smaller x the $R_{Fe}(x)$ has a plato or broad maximum at $R_{Fe} \simeq 1.05$ and does not follow the linear increase seen by the EMC. Within the errors the $R_{Fe}(x)$ has the same x-dependence as the similar ratio for nitrogen and deuterium targets, the $R_{N_2}(x)$. This indicates that the EMC effect has very weak dependence on the atomic number.

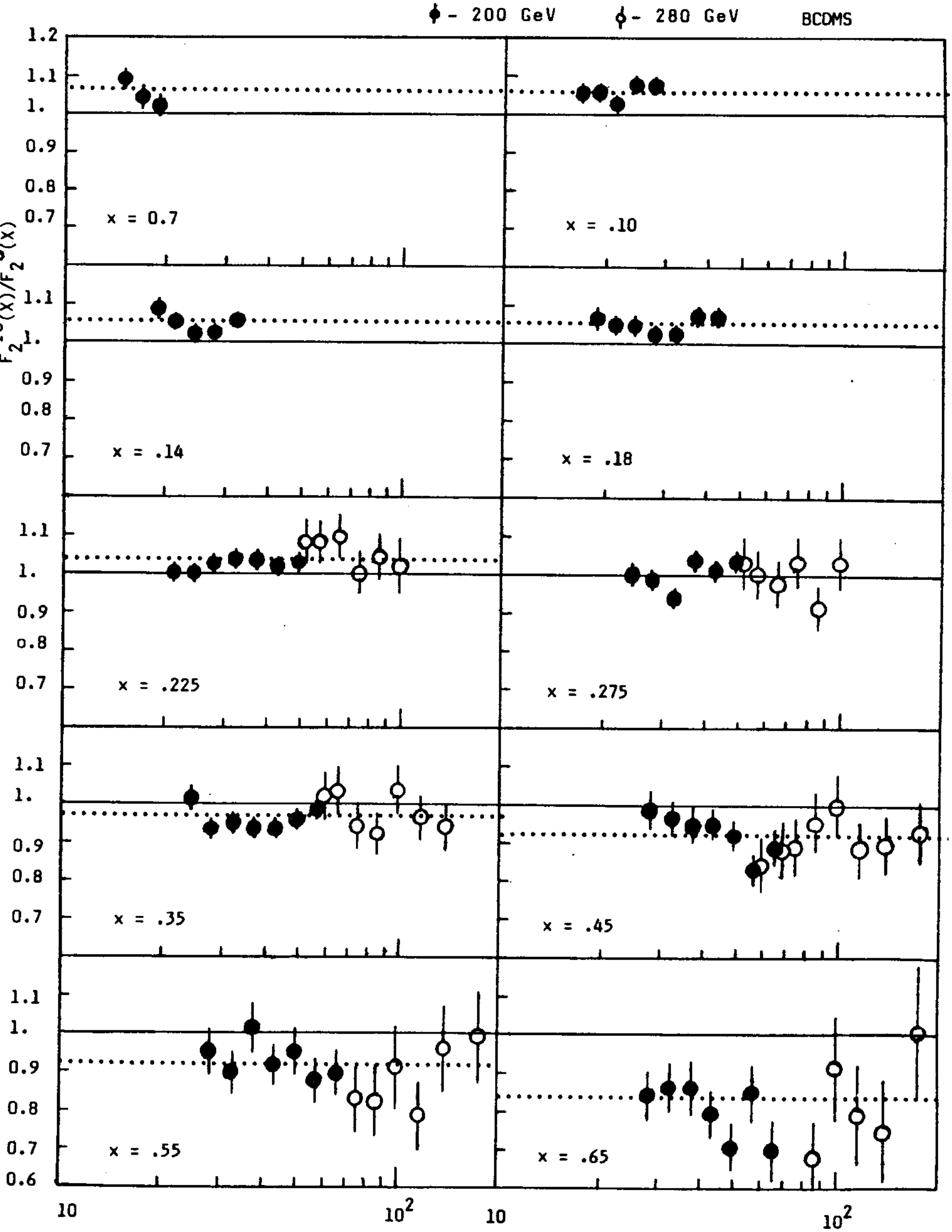

Fig. 6.

$F_2^{Fe}(X, Q^2) / F_2^D(X,Q^2)$ (NA-4).

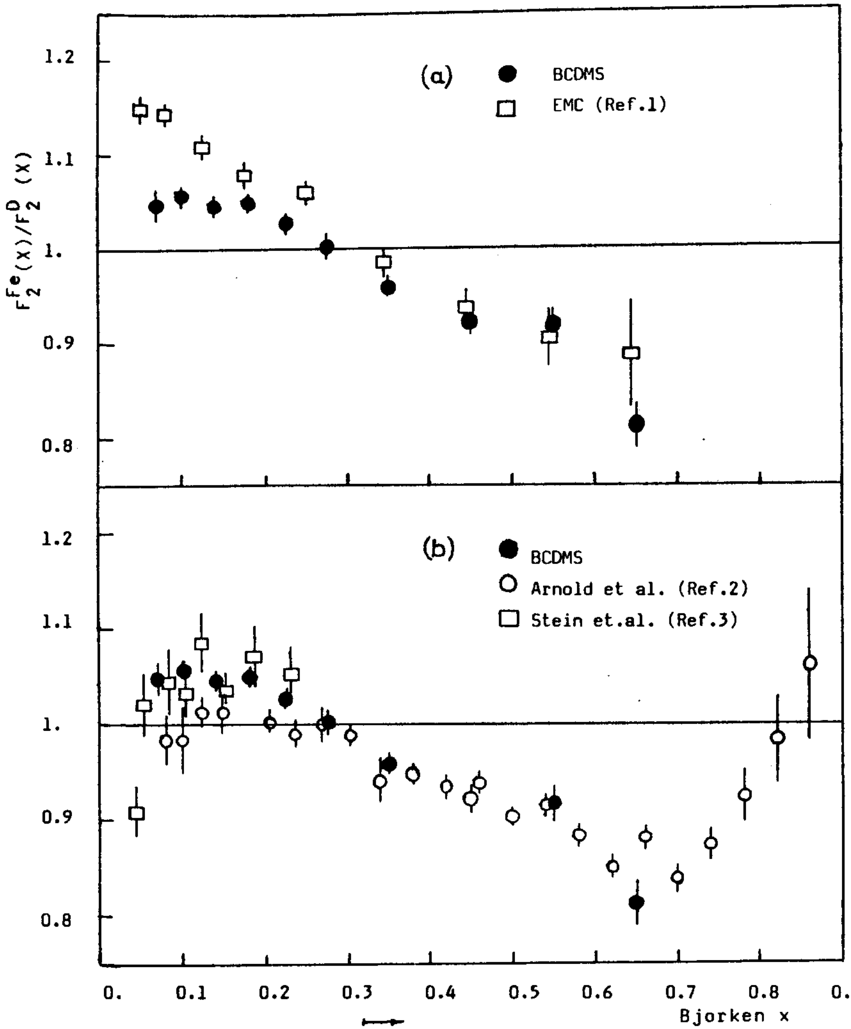

Fig.7·EMC effect in Fe/D_2 (NA-4)
For BCDMS: stat.errors 1÷3%
syst.errors 1÷4%

- Final results are obtained on nucleon structure functions $F_2(x,Q^2)$ measured from muon-carbon deep inelastic scattering. After detailed study of the apparatus resolution properties, calibration and development of the appropriate methods of the analysis the kinematic region x=0.25-0.8, Q^2=25-280 GeV is determined where the systematic errors are well under control and statistics is about $0.7 \cdot 10^6$ events at

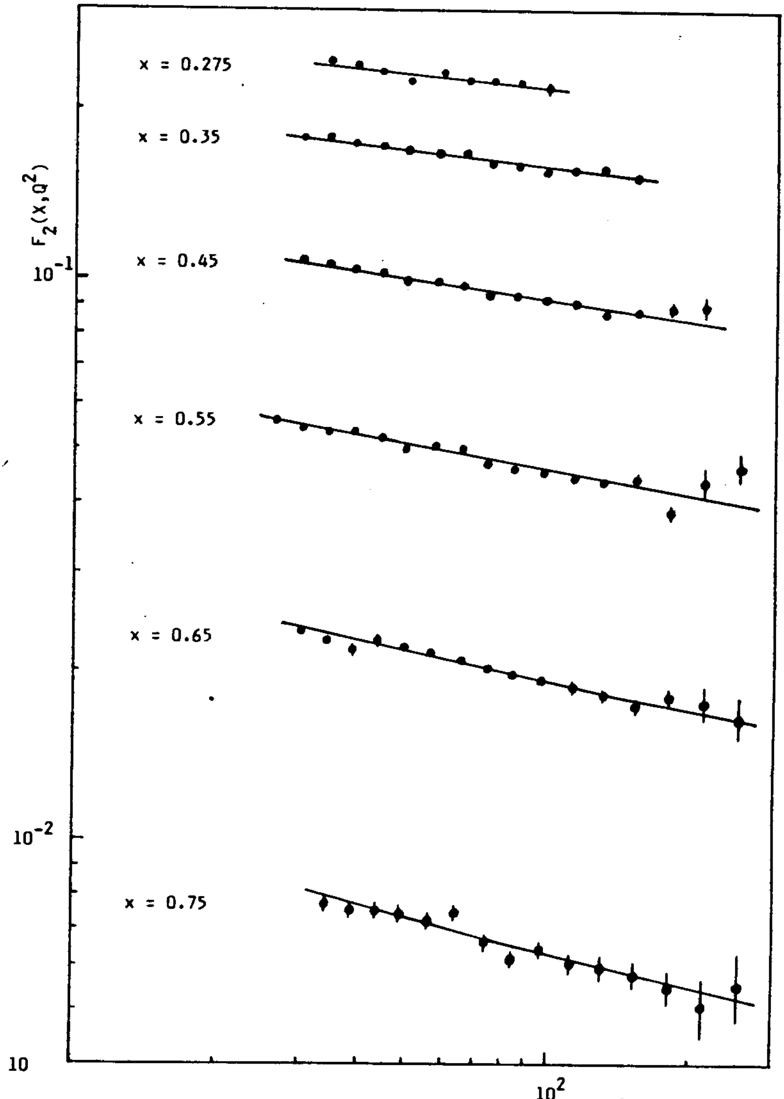

Fig. 8.

Collaboration BCDMS. Combined data $\mu + c \rightarrow \mu' + x$ at 120, 200 and 280 GeV ($0.7 \cdot 10^6$ events). Solid lines - QCD nonsinglet fit with $\Lambda_{\overline{ms}} = 230 \pm 20$ (stat) ± 60 (syst).

Fig. 9.

Logarithmic derivatives compared to QCD. Solid lines are QCD predictions for the $\Lambda_{\overline{MS}}$ determined from each experiment.

The EMC and BFP data desagree with QCD.

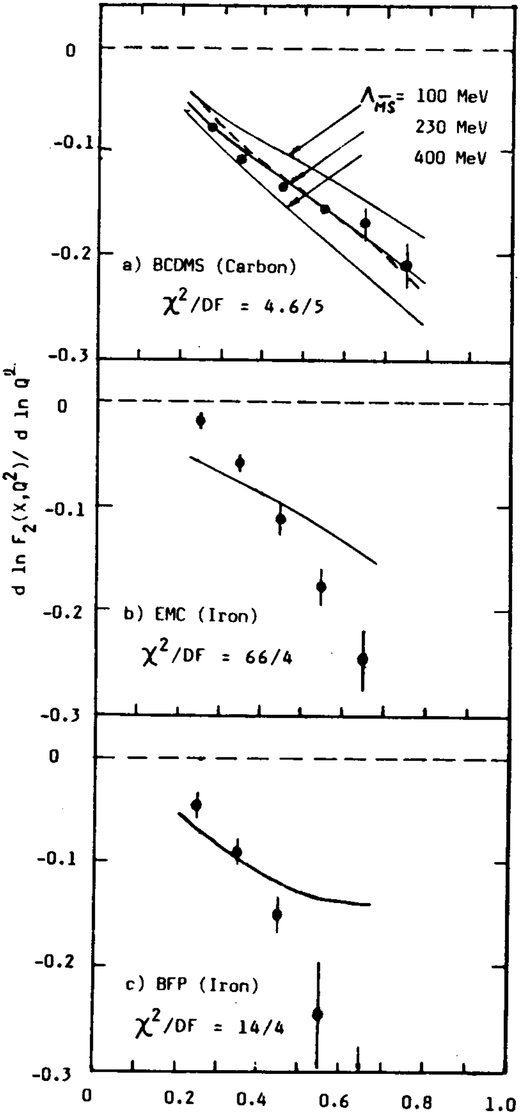

three energies of 120, 200, 280 GeV. Scaling violations clearly seen in $F_2(x,Q^2)$ as a function of Q^2 are analysed in terms of perturbative QCD (Fig.8). For this purpose two methods developed within the collaboration are used. The first one developed at Saclay (France) is based on a numerical solution of the Altarelli-Lipatov-Parisi evolution equation and requires for running a supercomputer. The second one developed at

JINR is based on the expansions of structure functions in Jacobi polynomial series. The methods allow to analyse the singlet and nonsinglet structure functions both in a leading and next-to-leading order of the perturbative QCD in the $\overline{MS}$ renormalization scheme. A good agreement of the data and QCD is obtained by both methods with $\chi^2/DF = 174/150$ and mass scale parameter $\Lambda_{\overline{ms}} = 230 \pm 20(\text{start}) \pm 60(\text{syst})$ MeV. A logarithmic derivative $d(\ln F_2)/d(\ln Q^2)$ as a function of x determined from data also agrees with the expectations from QCD (Fig.9). This is observed for the first time.

- Preliminary results are obtained on a high statistics measurement of the proton structure functions $F_2^P(x,Q^2)$ and parameter $R(x,Q^2) = \sigma_L / \sigma_T$ which characterize the ratio of the absorption cross sections for virtual photons with a longitudinal and transversal polarization. The analysis is based on $2 \cdot 10^6$ events after all cuts recorded at beam energies of 100, 120, 200 and 280 GeV and covered a kinematical range $x=0.06 \div 0.8$, $Q^2 = 7 \div 260$ GeV^2. This statistics is the biggest in the world. Scaling violations which are observed in data at all energies can be compared to the perturbative QCD predictions. Good agreement is obtained for a mass scale parameter of this theory $\Lambda = 210 \pm 20$ MeV using the both above mentioned programms. Also the gluon distribution parameter η (SO) was determined for the first time from the QCD analysis of singlet distributions accounting next-to-leading order corrections: η (SO) = 9 ± 1.5. This value is significantly larger than one in leading order (η (LO) $\simeq$ 5).

The x-behaviour of the parameter $R(x,Q^2) = \sigma_L/\sigma_T$ is also in good agreement with expectations from QCD.

- Data analysis of the NA-4 experiment is in progress. Nucleon structure functions measured from deuterium targets are being determined. Combining them with measurements from hydrogen targets neutron structure functions are to be obtained. The analysis of structure functions will be extended to the region of larger x.

3.3. The DELPHI experiment

The JINR specialists participate at the production, testing and assembling of streamer detectors for the Hadron Calorimeter (HC) of the DELPHI experimental set-up.

The detectors of the HC are tested in the beam of the Dubna synchrophasotron. The more reliable mode of the detectors operation is tested on-line to the computer. The preliminary work to the testing of the fullscale prototype of the HC at the phasotron beam has been done. A great amount of work to create and adjust the programmes of data modelling and processing is also performed.

The production of streamer detectors was finished in October 1987.

3.4. The USSR-JINR-USA-Poland-Bulgaria joint experiment at FNAL

The joint neutrino experiment E-564 is performed at the FNAL machine by using the method of nuclear emulsions placed inside the 15-inch bubble chamber of FERMIlab. 12 events of charmed particles were recorded. The charmed $\Sigma_c^{\bullet}$ (2450) baryon and two new types of the Λ_c^+-baryon decays were indentified for the first time. It was found that the most charmed Λ_c^+-baryons were produced in the cascade decay of Σ_c-baryons into Λ_c^+-baryon and π- meson.

4. RELATIVISTIC NUCLEAR PHYSICS

The relativistic nuclear physics is assumed to study quark -gluonic structure of nuclei. The Dubna scientists started to develop this new field of physics since 1970. At present new interisting results have been obtained which modified considerably the traditional conceptions on the nuclear structure.

The conventional model of the nucleus as a system of protons and neutrons is explained in the framework of the nonrelativistic quantum mechanics and describe the great amount of experimental facts. The first effect that could not be explained was the cumulative effect.The particles are produced in the region of nuclei fragmentation beyond the limits of the single nucleon collision kinematics. This effect was predicted by A.M.Baldin and experimentally confirmed by V.S.Stavinsky and his group in 1971 in the reaction d + Cu $\rightarrow$ π^++ ... at the energy of the primary deuteron beam of 4.5 GeV per nucleon obtained at the Dubna synchrophasotron at that time. The pions with the energy exceeding considerably the kinematical limit was observed for the case when isolated nucleons of the accelerated nucleus of deuteron interacted with a target.

A large amount of experimental information was obtained and analysed since the time of the cumulative effect discovery. The number of inclusive reactions

$$I_{(\gamma, \nu, \pi, p, d)} + \overline{II}_{(D, \dots, U)} \longrightarrow 1_{(\pi^\pm, K^\pm, p, n, \tilde{p}, d, t, He)}^{+} \cdots$$

were analysed within the energies up to 400 GeV. These experiments were performed at JINR, IHEP (Protvino), ITEP (Moscow), Erevan Physical Institute, Leningrad Institute of Nuclear Physics, at Fermilab and Berkeley Laboratory (USA). Data on cumulative particle production in the deep inelastic μ-scattering on nuclei at four transferred momenta $Q^2 \sim 100$ GeV^2 were obtained in the joint CERN-JINR NA-4 experiment, mentioned above. A quite big amount of film data was obtained and analysed at JINR in order to investigate main laws of the multiparticle production in the relativistic hadron-nuclei and nucleus-nuclei interactions.

4.1. Some principle results of the cumulative effect investigations

The cumulative effect can be considered as an evidence for the hadron matter "droplets" available in nuclei. These multiquark configurations differ strongly from the free nucleons. A.M.Baldin proposed a very simple fragmentation model according to which the cross section of the nucleus fragmentation to the meson, as well as the deep inelastic scattering cross section of leptons on the nucleus, are proportional to the quark-parton structure function of the nucleus. This supposition is based on the fact that quarks can be considered as quasi free particles at large four velocity transfers.

In experiments carried out at the JINR synchrophasotron the production of $\pi^{\pm}$ and $K^{\pm}$ mesons on more than 20 nucleus-targets interacting with the 9 GeV protons and deuterons at the angles close to 180^{0} was studied in details.

The mesons were recorded in the range of energies from 125 MeV/c to 1.2 GeV/c. The low limit of cross sections obtained in the experiment was:

$$\frac{I}{A} \; E \frac{d\sigma}{d\bar{p}} \sim 5.10^{-36} cm^{2} \cdot GeV^{-2} \cdot cp^{-1}.$$

The following properties of the structure functions $G(X,P^2)$ were determined (note that X is the scale variable, $0 \leq X \leq A$, and the cumulative effects corresponds to $X > 1$):

1. In the region of $0.6 \leq X \leq 3.5$ the structure function $G(X,P^2)$ is universal for various nuclei and can be approximated by the expression (see Fig.10)

$G(X,0) = \text{Const} \cdot A_{g}^{m(X)} \exp\left[-X/\langle X\rangle\right].$

For medium and heavy nuclei $\langle X\rangle \simeq 0.14$ within 10% accuracy. The value of the power is $m(X) = \frac{2}{3} + X/3$ for $0.6 \leq X \leq 1$ and $m(X)=1$ at $X > 1$ and $A_g > 20$.

II. The ratio of the nucleon normalized cross sections of pion on the Pb nucleus relatively to the cross section production of pions on the D, He, Al nucleus (Fig.11) was confirmed in the EMC and SLAC experiments on deep inelastic scattering of leptons on nuclei. JINR data at $X > 1$ may be considered as the prediction for the further experiments on deep inelastic scattering of leptons on nuclei.

III. The A-dependence of cross sections in the cumulative production shows that in all light nuclei up to $A_g \simeq 20$, the multiquark configurations differ from each other and from multiquark configurations in nuclei with $A > 30$. Data presented in Fig.12 are obtained at the value of $X = 2.1$, that is in the region of kinematical variables where the contibution of 9q and 12q-configurations is dominant.

IV. It was found that at similar X relation the approximative equality of cross section $E_1\frac{d\sigma}{d\bar{p}}(\pi^+) \simeq E_1\frac{d\sigma}{d\bar{p}}(K^+) \simeq E_1\frac{d\sigma}{d\bar{p}}(\pi^-)$ holds for $\pi^{\pm}$ and K^+. It confirmes the model of the quark stripping.

Recently a new series of experiments were carried out in order to measure cross sections of the kaon production on the lightest (d, He) nuclei. The structure function G(X) proved to be similar to quark-parton structure functions obtained for the pions and K^+ mesons, but its absolute value makes up 5% from G(X) in case of $\pi^{\pm}$ and K^+ mesons. This agrees satisfactorily with the quark mechanism for cumulative processes: K^+ and $\pi^{\pm}$- mesons are formed of valence quarks which enter into colliding objects, but K^- mesons are not.

Experimental data on the ratio of outgoing K^+/K^- (see Fig.13) do not confirm the generally adopted opinion that sea quarks have more "soft" distribution. This indicates the availability of a "hard sea" in the nuclei structure functions in the region of X from 1 to 2.5.

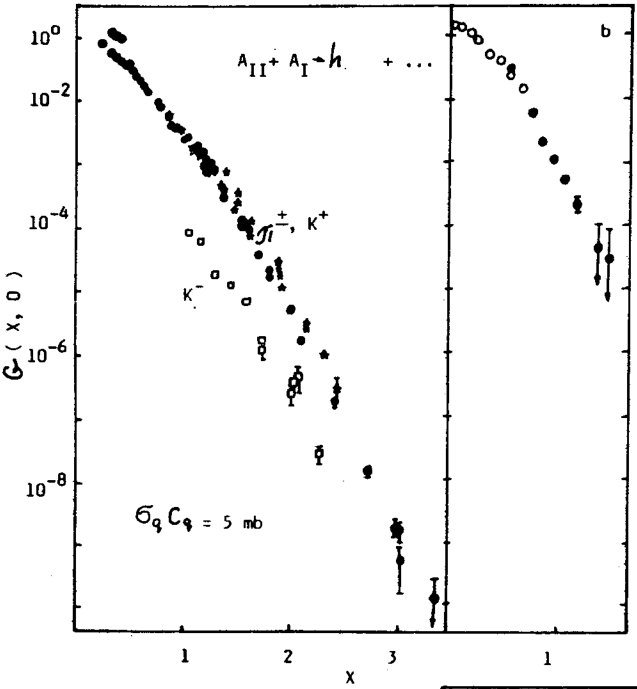

Fig.10. Left: cumulative hadron production; Right: deep inelastic μC-interaction. Parametrization $G(x,0)=\mathrm{const}\ A_{II}^{m(x)} \times$
$\times \exp\left[-x/\langle x\rangle\right]$
$\langle x\rangle \simeq 0,1$

$$m(x)=\begin{cases}\frac{2+x}{3}; & 0.6 \leq x \lesssim 1\\ 1; & x > 1\end{cases}$$

$A_{II} > 20$.

Fig. 10.

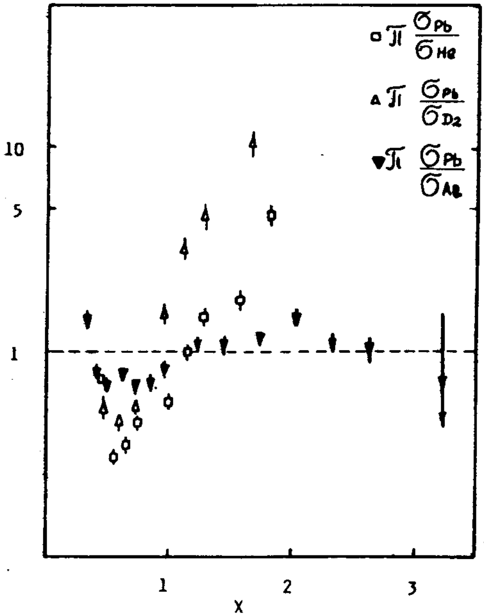

Fig.11. The ratio of the nucleon normalized cross sections of pion on the Pb nucleons relatively to the cross section production of pions on the D_2, He, Al.

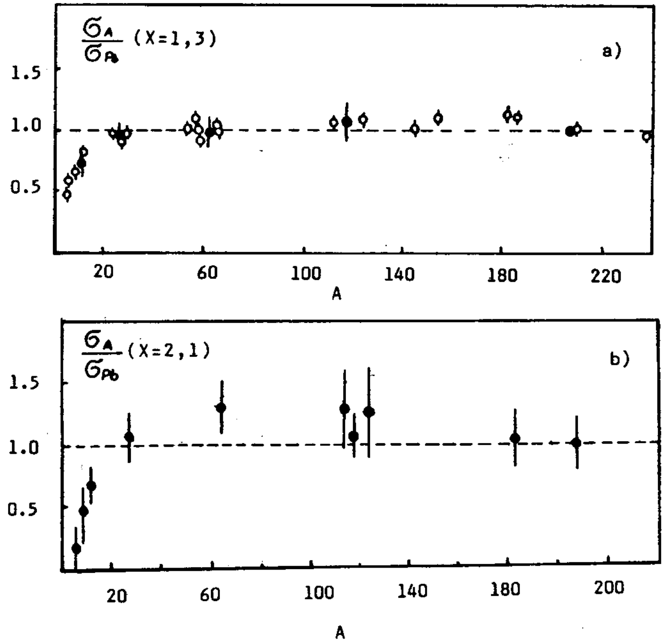

Fig. 12.
The A-dependence of cross-sections
in the cumulative production.

4.2. The boundaries of the nucleus proton-neutron model applicability and quark observation

To investigate nuclear processes in the relativistic region a mechanism of multiparticle production ($1+II \to 1+2+3$) in the space of relative 4-velocities b_{ik} was proposed:

$$b_{iK} = -\left(\frac{E_i}{m_i} - \frac{E_K}{m_K}\right)^2 + \left(\frac{\vec{P}_i}{m_i} - \frac{\vec{P}_K}{m_K}\right)^2 = -\left(u_i - u_K\right)^2,$$

where E_i, E_k are particle energies, $\vec{P}_i$, $\vec{P}_k$ are momenta, m_i, m_k are the masses of the follows: $E_i^2 - \vec{P}_i^2 = m_i^2$ or $u_{io}^2 - \vec{u}_i^2 = 1$.
It is possible to measure all b_{ik} for all charged particles using track sensible detectors. For the neutral particles parameters b_{ik} can be determined by the decays or secondary interactions of these particles.

When composite objects such as atom nuclei are in collision, the value of the 4-momenta transferred cannot be used as the criterion of the transition from quasiparticles nucleons to quasiparticles quarks. For example, in the case of the relati-

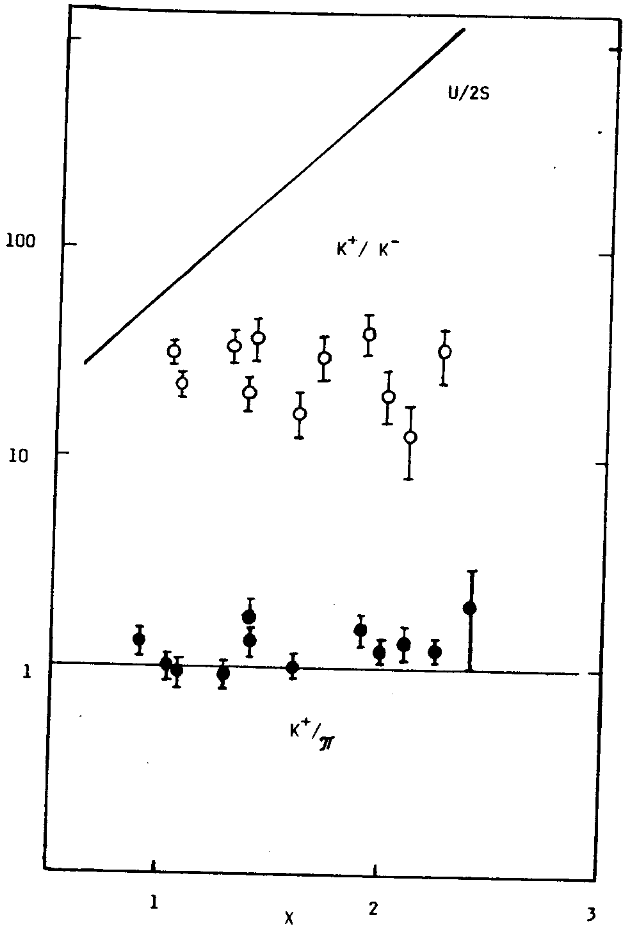

Fig.13.
Experimental data on the ratio K^+/K^- .

vistic nucleus stripping the huge 4-momenta transfer takes place. But this transfer is due to the large mass of interacting objects and is not related to the excitation of coulor degrees of freedom.

The classification of nuclear interactions by using b_{ik} variables was proposed in 1975 at the Santa Fe Conference: $b_{ik} \leqslant 10^{-2}$ corresponds to the region where the proton-neutron model is valid, $b_{ik} \gg 1$ corresponds to the region where the quark-gluon interaction is predominant, and $b_{ik} \sim 1$ corresponds to the reorganization of the inner structure of hadrons when resonances, hyperons production takes place.

The experiments performed at JINR demonstrated that at $b_{ik} \gtrsim 5$ the interaction among quarks entering into the i and k objects is weakened so that it can be treated on the base of the perturbation theory. To collide the relativistic nucleus (I) with the nucleus at rest (II) the boundary of $b_{ik} \approx 5$ is attained at $E_I = 3.5 \div 4 \cdot A_I$ GeV. This corresponds to the start of the asymptotic mode of the nuclei limiting fragmentation (approximative scale invariance). There was a possibility to get nuclei at the JINR synchrophasotron with the energy above this boundary that allowed Dubna physicists to formulate new laws defining the properties of the highly excited nuclear matter.

The cross section of the multiparticle production taken in b_{ik}-variables can be expressed as:

$$\frac{d\sigma}{\prod d b_{ik}} = W(b_{I\,II}, b_{I1}, \ldots, b_{ik}, \ldots). \qquad (2)$$

In the case of asymptotically large b_{ik} the probabilities (2) have to possess the properties of the automodelity (V.A.Matveev, R.M.Muradian, A.N.Tavkhelidze) according to $b_{\alpha\beta}$:

$$W(b_{\alpha\beta}, b_{\alpha i}, b_{\beta i}, b_{ik}, \ldots) \rightarrow \frac{1}{(b_{\alpha\beta})^m} W\left(b_{\alpha i}, \frac{b_{\beta i}}{b_{\alpha\beta}}, b_{ik}, \ldots\right). \qquad (3)$$

The main principle of the correlation depletion (N.N.Bogolubov) in the space of relative 4-velocities based on the generalization of experimental data (when the interaction of α and β objects is weakened at $b_{\alpha\beta} \rightarrow \infty$) shows that if all b_{ik} in (2) are divided into groups $\{\ldots, b_{ik}, \ldots\}_\alpha$ and $\{\ldots, b_{jn}, \ldots\}$, then in the asymptotic limit, when between i and k points b_{ik} from different groups tend to infinity, the probabilities W are presented in the following form:

$$W^{\alpha\beta} = W^{\alpha} \frac{1}{(b_{\alpha\beta})^m} W^{\beta}. \qquad (4)$$

The probabilities are factorized; one of the factors describes particles from the α group, the other one - from the β group.

Numerous experimentally obtained laws common as to the relativistic nuclear physics and high energy physics hadron processes satisfy the general structure of the expression (4). The limiting fragmentation, diffraction dissociation, Regge models are the particular case of the correlation depletion principle in the form of (4). The considerably new application of the correlation depletion principle is a conception of relativistically invariant determination of jets-sharply oriented emission of hadron matter in the particles nuclei collisions. Using the b_{ik} approach jets can be explained as relativistically invariant clusters W^{α}, W^{β} etc. In 1984 data on π^--C interactions at the 40 GeV/c incident pion momentum were analysed. These data were obtained when 2 meter propane chamber was irradiated at the IHEP PS. The identity of jets produced in the frgamentation region of the carbon nucleus and pion is demonstrated in Fig.5. More than 300 000 of events of a broad spectrum (pp, $\bar{p}$p, πp, πC, pC, pTa, $\tilde{\nu}$N) in the region of energies from 6 to 205 GeV were analysed. It was found that the hadron distributions (π^-, K^0_s, Λ^0) by b_{ik} relative to the jet axis at the momentum of $P_{lab} \geq 22$ GeV/c and $\sqrt{S} \simeq 6$ GeV did not depend on the energy and on the type of the fragmentating system (hadron, nucleus).

The independency of the jet properties of their production and their universal character, allows one to interpret this as the result of the colour charge interaction with vacuum.

There is an opinion that colour objects - quarks, gluons - are not observable because they interact immediately with the vacuum fluctuations transforming into hadrons. However, it is obvious that this process is not momentary and the ultimate length to form the quark into hadron exists. The particles which are not stable relatively to strong interactions (ρ-mesons, Δ and so on) are assumed as observable. This fact is based on two main criteria:

a) the cross section of σ can be presented with a sufficient accurancy in the form of $\sigma = \sigma_p W_d$ where W_d is the probability of the decay or secondary interaction; σ_p is the production cross section

b) the universality of W_d, independence of W_d of the reaction type, the relativistic invariance of W_d.

Nobody succeded to see unstable particles in the experiments, but the properties of W_d are trustfully registered and this serves as reliable criteria to reconstruct even extremely unstable particles .

The properties of quarks and gluons can be determined by analogy to the properties of invariant and universal jets. The fact that quarks are observed is in agreement with the a) and b) criteria. The universal character of jets mentioned above guarantees that quarks and gluons exist for a suffucient time to cover the distance longer than the dimensions of the parent system.

The angular and energy characteristics of the axis distributions must be described by QCD that agrees with the experiment.

On the base of this consideration it is possible to suppose that the attempts to obtain the equillibrium quark gluon plasma at very high energy nuclear collision (for example at CERN machines) would not be successful. The W distributions will be divided into clusters depending on $b_{I\ II}$ and the influence of the nuclei properties on the jet production will be the same as was shown above. The existence of "fireballs" isotropically decaying in their system of rest is doubtful since W^{α} and W^{β} depend also on the direction segment connecting U_{α} and U_{β} points.

The investigation of the cumulative effect and various aspects of the correlation depletion principle, especially hadron jets, will be continued.

4.3. Experimental methods and facilities for the investigations in the relativistic nuclear physics

Relativistic nuclear physics is concerned with high energy physics. The main facilities of investigations in this region are modified synchrophasotron and sophi-

Table 5

EXPERIMENTAL FACILITIES FOR RESEARCH IN RELATIVISTIC NUCLEAR PHYSICS LOCATED IN THE SYNKHROPHASOTRON AREA

2 m propane bubble chamber Volume: 210x65x43 cm^3; magnetic field: H = 15.5 ke; $\frac{\Delta p}{p}$ = 5-12%.	Study of interactions of relativistic nuclei and neutrino with light and heavy nuclei for a search of multiquark states
ALPHA 3C Proportional and drift chamber magnetic spectrometer + time flight and ionization hodoscopes; $\frac{\Delta p}{p}$ = 0.3%; $\Delta\theta$ = 0.8 mrad	Search of highly excited states of the few nucleon systems in experiments on scattering and fragmentation of relativistic nuclei. Deuteron wave function was measured in the reaction
Recoil Particle Spectrometer semiconductor telescope; gaz identificator; scintillation magnetic spectrometer in the internal beam of the accelerator	Study of the p, ^3He, ^4He, ^6He, ^6Li, ^7Li in the 6.6 GeV proton interaction with nuclei. Behaviour of structure functions at 6-400 GeV. Proof of the hypothesis of nuclear scalar invariance.
DISK 3 Cerenkov and scintillation counters $\frac{\Delta p}{\mu}$ = 6%; Time flight resolution - 1 nsec	Investigation of the particle cumulative production in the relativistic nuclear physics
130 channel Cerenkov Mass Spectrometer	Search and study of the resonance production and decay into e^+e^- pairs and γ-quanta
RESONANCE Streamer chamber with a liquid hydrogen target in the magnetic field	Search for 6 quark strange dibaryon systems
MASSPEAK Magnetic spectrometer with wire chambers	Study of nuclear interactions at relativistic energies. Search for multiquark states in nuclei
Hybrid Streamer Chamber Magnetic Spectrometer including vertex detector, system of the beam testing, fast processors, proportional chambers volume: 2x1x0.6 m^3; magnetic field of 1.5 tesla.	Study of the inelastic nuclei-nuclei collisions; compression of nuclear matter; search for abnormal superdense nuclei.

sticated detectors used in particle physics. Presently at JINR 4 track sensitive detectors and 7 large electronic devices are used in the experiments on relativistic nuclear physics (see Table 5). In comparison with the particle collisions the relativistic nuclear collisions produce very big multiplicities of secondary particles.

But from the point of view of the quark physics the region of asymptotically large b_{ik} and greater X ($\geqslant 1$) gives more information about rare processes with small cross sections. For these processes large multiplicities of particles in nuclear collisions are not of great importance. The main new condition to carry out experiments in relativistic nuclear physics is the availability of intensive particle beams. In this connection JINR gives consideration to the development of the accelerator facilities. The acceleration of deuterons in 1970 and afterwards of helium nuclei did not require great modifications of the synchrophasotron. The advancement in the study of heavier nuclei was realized after the creation of the highly charged ion sources, reconstruction of the injector, high frequency and vacuum systems, etc. Three types of the original sources of ions or nuclei was developed and put in operation: the cryogenic electron beam source (E.Donetz), lazer source and "Polaris" - the polarized deuteron source. The slow ($\sim$ 500 msec) and fast ($\leqslant 1$ msec) extraction systems were realized and 12 beam lines were formed to carry out experiments at the Dubna synchrophasotron the main characteristics of which are presented in Table 6:

Particles	Energy (GeV)	Intensity (p.p.c.)	Particles	Energy (GeV)	Intensity (p.p.c.)
p	9	4×10^{12}	$_{7}Li^{3+}$	23.9	4×10^{9}
d	8.2	1×10^{12}	$_{12}C^{6+}$	49.2	2×10^{9}
d↑	8.2	1×10^{9}	$_{16}O^{8+}$	65.6	5×10^{7}
n	9	1×10^{10}	$_{19}F^{9+}$	73.1	1.5×10^{7}
$_{3}He^{2+}$	17.2	2×10^{10}	$_{22}Ne^{10+}$	81.0	10^{4}
$_{4}He^{2+}$	16.4	5×10^{10}	$_{24}Mg^{12+}$	98.4	3×10^{7}
$_{6}Li^{3+}$	24.6	1.5×10^{8}	$_{28}Si^{14+}$	114.8	3×10^{4}

At present in Dubna a new superconducting strong-focusing synchrotron is under construction. This type of the accelerator is called NUCLOTRON. The 6-7 GeV/nucl. machine will provide a sufficient increasing of the mean intensity of beams, a possibility to accelerate nuclei up to uranium, improvement of beam quality, of their spatial and time-depended characteristics.

A tunnel to install the magnet system of the NUCLOTRON is prepared; modules of the magnet system and other systems are manufactured. The main mounting works will be accomplished by the end of 1988. Meanwhile the synchrophasotron operates normally, approximately $\sim$ 4000 working hours per year.

NUCLOTRON will provide the greater possibilities to carry out experiments on the investigation of relativistic nuclear collisions. Besides the above mentioned study of hadron jets and cumulative effect, the search for particles which are not described by standard quark schemes will be continued, as well as the study of various manifestations of the confinement, quantum chromodynamics of large distances, problems of hypernuclear physics, etc.

Hence, the investigation of relativistic nuclear collisions gave a principally new approach to the conception of nuclear structure determined the boundaries of the proton-neutron nucleus model applicability. It is evident that the study of the quark degrees of freedom of atom nuclei in nuclear reactions is of a fundamental importance and gives broad perspectives in nuclear physics research. The relativistic nuclear physics, as a large part of the microcosmos physics, is and will be rapidly developed.

5. PARTICLE PHYSICS EXPERIMENTS CARRIED OUT AT PULSED REACTORS AND OTHER JINR FACILITIES

5.1. The electrostatic beta-spectrometer to determine tha mass of the neutrino

At the JINR laboratory of Nuclear Problems an experimental set-up is created to determine the mass of the neutrino. It has the record energy resolution

$\Delta E \sim 3$ eV in the region of $E_e \sim 10\text{-}20$ KeV.

By using this spectrometer the direct measurements of the natural widths of the Thulium atomic levels were measured for the first time. There were used low energy electrons of the inner conversion from the ^{169}Yb (Ytterbium) decay. The latter was used as the calibration source to determine the mass of the neutrino. If the natural width is not accounted in experiments with Tritium, the mass of the neutrino is "generated", the value of which would be approximately 20 eV at the true zero meaning and the spectrometer energy resolution is $\Delta E \sim 45$ eV.

5.2. Experiment to determine the electric charge of the neutron by using ultracold neutrons

In 1986 the first period of the experimental research to determine the electric charge of the neutrons with the help of the ultracold neutron installation was finished. The principle of the measurement was the deflection of the neutron beam in the electric field. In comparison to the installations operating by using hot and cold neutrons the ultracold neutron facility had a significant benefit in sensibility due to very low energy of ultracold neutrons. Methods of neutron optics were applied to realise this experiment. This installation operates by focusing the ultracold neutron beam with the help of the vertical cylindrical mirror.

The main part of this installation is the neutron-optic chamber manufactured at the Laboratory of Neutron Physics and mounted in the ultracold neutron beam of the Leningrad Nuclear Physics Institute reactor VVR-M. The density of UCN flux was $6 \cdot 10^3$ neutron/cm^2:sec. The layout of the installation is shown in Fig. 14.

Neutrons are passing through the entrance grating, reflecting from horisontal mirrors (2) and cylindrical mirror (4) and focusing in the plane of the entrance grating. The radius of the mirror curvature is 1041 millimeter; the distance between horisontal mirrors is 50 mm. Mirrors are coated by BeO, 2000 A trick, with a limiting velocity of 7 m/sec. The entrance grating slits are 0.7 x 50 mm. The cylindrical mirror provides the neutron optic image of the slits in the plane of the grating which consists of two parts moving relatively each other. Neutrons passed through each part of the entrance grating are registered in separate detectors(6) by a double exit neutron-guide (7). Thus, while the grating is moving along the X axis (see Fig. 14), the counting of detectors is changed (see Fig.15).

The electrodes (3) provide the input of the high voltage electric field. By measuring the shift of ultracold neutron beam it is possible to evaluate the electric charge of the neutron. For this purpose the grating has to be set at the point A (Fig.15). One of the detectors counts ultracold neutrons in the left slope of the

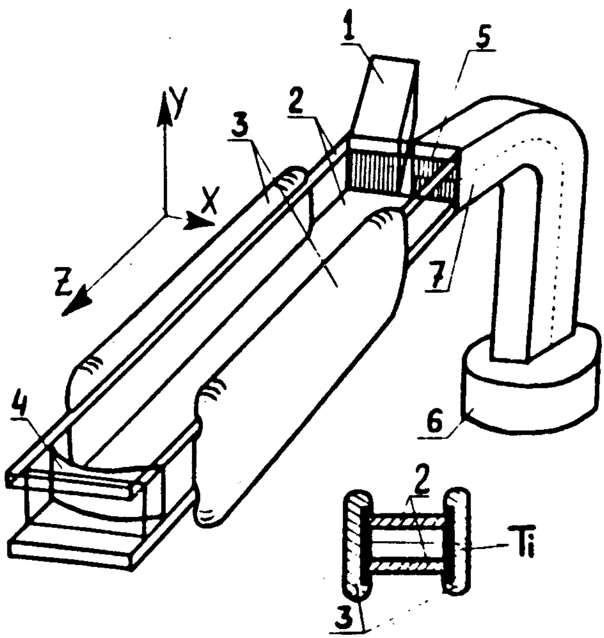

Fig.14·

The layout of the installation (UCN).

beam, the other one - in the right slope of the beam; the changes in the counting connected with the shift of the neutron-optical image are being registered.

High voltage power source provides the 10 Kv/cm electric field. The sensitivity of the installation is determined by the peak curvature and neutron time flight through the abscissa axis.

To determine the sensitivity the measurements of the neutron spectrum by time of flight along the installation were made, as well as the calibration in the gravitation field of the Earth. The sensitivity was equal to that of the installation to measure the neutron electric charge on ultracold neutrons at the reactor of the Laue-Langeven Institute in Grenoble. In this case $q_n = 9\ 10^{-20} q_e$ per 24 h/measurement where q_e is the charge of the electron. In a serie of measurements the result $q_n \lesssim 7 \cdot 10^{-20} q_e$ was obtained. Thus, for the first time the result obtained earlier in Grenoble was confirmed: $q_n \lesssim 3 \cdot 10^{-20} q_e$.

The increasing of the installation sensitivity is connected with the improvement of the optic characteristics of the tract and the rise of the applied electric field.

5.3. The experimental determination of the mean square radius of the charge distribution in the neutron. The electric polarizability of the neutron

The mean square radius $\langle r_{in}^2 \rangle_n^{1/2}$ of the charge distribution in the neutron is the fundamental characteristic of the neutron structure which provides an

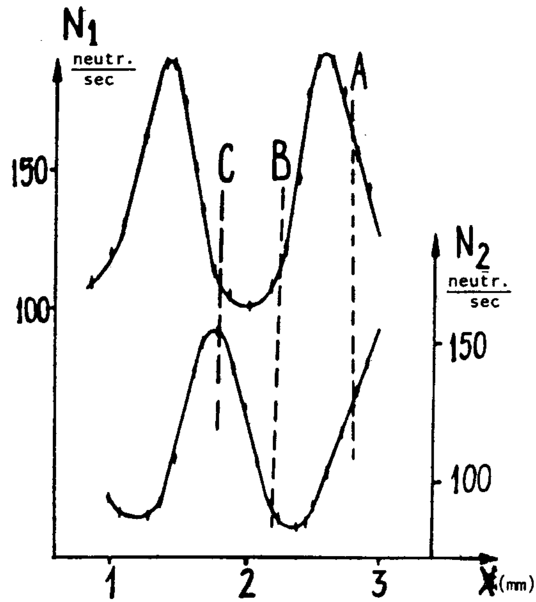

Fig. 15.

By measuring the shift of ultracold neutron beam it is possible to evaluate the electric charge of the neutron.

important test of the contemporary theoretical notion. Let us mention about the model of the chiral "bag",etc. The value of $\langle r_{in}^2 \rangle_n^{1/2}$ can be obtained from the experiments on electron scattering on deuterons. But the most reliable information about this value is the scattering of very slow neutrons on heavy atom electrons. It was shown by Foldy that

$$\langle r_{in}^2 \rangle_n = \frac{3\hbar^2}{M_e^2} \left(a_{ne} - a_F \right), \qquad (1)$$

where a_{ne} is the measured length of the (ne) - scattering, $a_F = \mu_n \frac{e^2}{M_c^2}$ and the member a_F =-1.468 x 10^{-3} fm is not associated directly to the inner structure of the neutron.The value of $a_{ne} \simeq 1.5\times10^{-3}$fm is almost 10^4 times lesser than the length of the nuclear scattering and the contribution of the (ne) - scattering does not exceed few percent portions.

To determine a_{ne} two experiments were carried out not connecting by the methods used. One of them was performed to investigate the neutron diffraction reflection from the tungsten single crystals enriched by the ^{186}W isotope the nuclear scattering of which is strongly suppressed.Due to this the relative contribution of the (ne)scattering is sufficiently increased up to 15-20%.In the second experiment the energy dependence of the neutron bismuth cross section was measured in the range of energy 1-100 eV. The results obtained agree between each other and its averaging gives $\langle r_{in}^2 \rangle_n^{1/2}$ =(-0.11$\pm$ 0.02)fm where the minus sign corresponds to $\langle r_{in}^2 \rangle_n < 0$. This value differs from the analogous ones obtained at Argonne, Brookhaven,Garching ($\langle r_{in}^2 \rangle \gtrsim 0$). In the experiments performed at these laboratories the (ne)-scattering did not exceed 1-2% and data processing was not correctly made. The values of $\langle r_{in}^2 \rangle_n \gtrsim 0$ obtained at these laboratories did not find a theoretical interpretation in not a single nucleon model. Calculations proceeded within the chiral bag model give the value $\langle r_{in}^2 \rangle_n^{1/2} \simeq -0.3$ fm that agrees qualitatively with results obtained in Dubna Laboratory of Neutron Physics.

The second important property of the neutron structure is the electric polarizability of the neutron which is studied by the methods of low energy neutron physics. The upper limit of the electric polarizability coefficient was obtained $\alpha_n < 5 \times 10^{-3} fm^3$ in the reaction with bismuth. This value is the best for today.

In this review I have considered only few aspects of the scientific program of JINR in the particle physics. Future investigations are related mainly to the constructions of such machines as the UNK Accelerator Storage Complex in Serpukhov, LEP Collider at CERN, the superconducting relativistic accelerator NUCLOTRON in Dubna.

I am grateful to Drs Kovalenko A.D., Sapoǎhnikov M.G., Govorov A.M. as well as Mrs. Savina G.N., Studenova M.V. and Sissakian N.I. for help in preparing these lecture notes.